Creation and manipulation of entanglement in spin chains far from equilibrium

F. Galve[1,3], D. Zueco[2,3], G.M. Reuther[3], S. Kohler[3,4], and P. Hänggi[3,a]

[1] IFISC (CSIC – UIB), Instituto de Física Interdisciplinar y Sistemas Complejos, Campus Universitat Illes Balears, 07122 Palma de Mallorca, Spain

[2] Instituto de Ciencia de Materiales de Aragón y Departamento de Física de la Materia Condensada, CSIC-Universidad de Zaragoza, 50009 Zaragoza, Spain

[3] Institut für Physik, Universität Augsburg, Universitätsstraße 1, 86135 Augsburg, Germany

[4] Instituto de Ciencia de Materiales de Madrid, CSIC, Cantoblanco, 29049 Madrid, Spain

Abstract. We investigate creation, manipulation, and steering of entanglement in spin chains from the viewpoint of quantum communication between distant parties. We demonstrate how global parametric driving of the spin-spin coupling and/or local time-dependent Zeeman fields produce a large amount of entanglement between the first and the last spin of the chain. This occurs whenever the driving frequency meets a resonance condition, identified as "entanglement resonance". Our approach marks a promising step towards an efficient quantum state transfer or teleportation in solid state system. Following the reasoning of Zueco et al. [1], we propose generation and routing of multipartite entangled states by use of symmetric tree-like structures of spin chains. Furthermore, we study the effect of decoherence on the resulting spin entanglement between the corresponding terminal spins.

1 Introduction

Interacting spins are ubiquitous in physics, whether it be in magnetic molecules [2], cold atoms [3], Penning traps [4] or Josephson-junction arrays [5]. Since years, the equilibrium and non-equilibrium properties of interacting spins have been extensively studied. Phenomena such as quantum and classical phase transitions and dynamical localization [6] are well-known in the literature. The Heisenberg, Ising, and XY coupling models became paradigmatic models in condensed matter physics and statistical physics [7].

Needless to say, the dynamics of interacting spins is of quantum nature. The interest in those systems has been reinforced along with new prospects in quantum technologies, which are expected to exceed dramatically the capabilities of their classical analogs. Typical examples are quantum metrology [8] or quantum information processing [9], with applications such as simulators or universal quantum computers. With the perspective of quantum computing in mind, spin chains are natural connectors of information between the different parts of the "quantum hardware" and the readout device [10–12].

A key ingredient for all these applications is the entanglement between different spins in an array. Entanglement has no classical analogue and marks the gap between classical and quantum technology. Coming back to quantum communication protocols, the entanglement shared by the emitter and receptor of the information ensures a communication superior to what would be possible with classical protocols [12]. Consequently, the ability to fully control

[a] e-mail: `hanggi@physik.uni-augsburg.de`

entanglement creation and manipulation is a fundamental requirement. One way to achieve this is by using time dependent fields. The benefits of external ac-driving has been recently reported in Refs. [1,13–18]. However, from a technological point of view, it appears rather difficult to access each spin separately by applying local magnetic fields.

In this work, we review and extend our recent results [1,13] for entanglement control via global external fields acting on all spins in an array. Concretely, we discuss entanglement creation between both ends of the chain, which turns out to be optimal at particular driving resonances. Once entanglement is created locally, neighboring spins interact such that the spins at the ends of the chain efficiently communicate with each other and entanglement routing through the chain remains the main task. Here, we extend former studies on entanglement creation via modulation of the spin-spin coupling [13] to the case where modulation of the local splittings is used instead.

In the second part of this work, we report our idea of quantum information routing by means of ac-fields. In detail, we propose a way to produce multipartite entanglement between many distant parties just by joining several "quantum routers" in "beam-splitter" mode. Finally, we provide studies on the validity of both driving protocols discussed above under decoherence.

The paper is organized as follows. In Sec. 2 we introduce the model and quantify the entanglement by means of the concurrence between the outermost spins of the chain. Section 3 is devoted to entanglement resonance, while in Sec. 4 we introduce the idea of routing and entanglement distribution in quantum networks. In Sec. 5 we discuss a possible implementation in Penning traps.

2 Driven spin chains and entanglement computation

In this work we describe a chain of N spins by the anisotropic XY-model with time-dependent parameters using the Hamiltonian [19] ($\hbar = 1$)

$$H = \frac{1}{2}\sum_{n=1}^{N} h_n(t)\sigma_n^z + \frac{J(t)}{4}\sum_{n=1}^{N-1}\left[(1+\gamma)\sigma_n^x\sigma_{n+1}^x + (1-\gamma)\sigma_n^y\sigma_{n+1}^y\right]. \tag{1}$$

Both the local energy splittings $h_i(t)$ and the interaction strength $J(t)$ are assumed to depend through modulated global fields acting on all spins at the same time. Nevertheless we allow for inhomogeneities of the fields. A non-zero value of the parameter γ refers to an homogeneous anisotropy. For possible applications in quantum communication the spin chain must have open ends. Both the isotropic limit of the model $\gamma = 0$ and the thermodynamical limit $N \to \infty$ can be solved analytically in the time-independent case by means of the Jordan-Wigner transformation [19,20]. On the contrary we are interested in both finite-size effects and time-dependent dynamics. We consider the fields to be composed of a dc contribution and one harmonic component, such that

$$h_n(t) = \epsilon_n(h_0 + h_1\sin\omega t) , \quad J(t) = J_0 + J_1\sin\omega t. \tag{2}$$

For later convenience we move to an interaction picture defined by $\widetilde{X} = U_0^\dagger(t)XU_0(t)$, where $U_0(t) = \exp[-i\sum_n \varphi_n(t)\sigma_n^z]$ and $\dot{\varphi}_n(t) = h_n(t)/2$. Introducing the ladder operators $\sigma^\pm = \frac{1}{2}(\sigma^x \pm i\sigma^y)$, the Hamiltonian (1) gets replaced by the interaction-picture Hamiltonian

$$\begin{aligned}
\widetilde{H} = \frac{1}{2}\big(J_0 + J_1\sin(\omega t)\big)\sum_{n=1}^{N-1}&\Big[\sigma_n^+\sigma_{n+1}^- e^{i\Delta_n(t)} + \sigma_n^-\sigma_{n+1}^+ e^{-i\Delta_n(t)} \\
&+ \gamma\Big(e^{i\Sigma_n(t)}\sigma_n^+\sigma_{n+1}^+ + e^{-i\Sigma_n(t)}\sigma_n^-\sigma_{n+1}^-\Big)\Big],
\end{aligned} \tag{3}$$

where $\Delta_n = \varphi_n - \varphi_{n+1}$ and $\Sigma_n = \varphi_n + \varphi_{n+1}$. The first two terms in the sum of Hamiltonian (3) swap the states of spins n and $n+1$, whereas the latter two terms create and destroy excitations,

respectively. As it will turn out, the swapping terms are responsible for entanglement transfer while the latter pair of terms constitutes the origin of entanglement generation.

In the following, we are interested in the bipartite entanglement between two spins in the chain. For this purpose one needs to obtain the reduced density matrix of spins j and k. It results from the full density matrix of the chain ϱ_{tot} by tracing out all other degrees of freedom,

$$\varrho_{jk}(t) = \text{Tr}_{n \neq j,k}\big[\varrho_{\text{tot}}(t)\big] \tag{4}$$

where $\text{Tr}_{n \neq j,k}$ denotes the partial trace with respect to all spins $n = 1, 2, \ldots, N$ but spins j and k. The entanglement shared by spins j and k is then given by the concurrence [21]

$$C_{jk} = \max\{\lambda_1 - \lambda_2 - \lambda_3 - \lambda_4, 0\}. \tag{5}$$

The λ_ν are the ordered square roots of the eigenvalues of the matrix $\varrho_{jk}(\sigma_j^y \sigma_k^y)\varrho_{jk}^*(\sigma_j^y \sigma_k^y)$.

3 Resonances and entanglement creation

The time dependence of the coefficients in the Hamiltonian (1) generally leads to a complex dynamics, in addition to the nontrivial dynamics for the time-independent case. Therefore, we confine ourselves to scenarios in which both amplitudes J_1 and h_1 from Eq. (2) are smaller than the dc field strength h_0. We focus on the spectral response of the chain to periodically modulated coupling. All other parameters have arbitrary but fixed values. For simplicity, we assume in this section a homogeneous chain, $\epsilon_n = 1$ for all n.

In the protocol, the spins are initially uncoupled, i.e. $J(t) = 0$ for $t < 0$, and cooled down to the fully-aligned separable state

$$|\psi(t = 0)\rangle = |0000\ldots\rangle, \tag{6}$$

which is the ground state of the Hamiltonian (1) with $J = 0$. At $t = 0$, we switch on both the coupling $J(t)$ and the sinusoidal driving $h(t)$. This procedure is termed a quantum quench and constitutes a typical protocol for entanglement generation [22]. Even though the interaction strength is usually considered as constant, we take into account the possibility of time-dependent coefficients $J_1(t) > 0$ for $t > 0$. In this sense we are introducing time-periodic quantum quench dynamics.

In the following, we raise the question of how much entanglement between the ends, measured in terms of the concurrence, may be created of the chain. Such large-distance entanglement could be used for typical quantum communication protocols, such as teleportation or state transfer [12].

3.1 Time-dependent interaction

At first, we only consider the interaction to depend on time, i.e. $h_1 = 0$ and $J_1 \neq 0$. We investigate the time evolution of the concurrence between spin zero ($n = 0$) and the last spin ($n = N$) for different driving frequencies ω_d, and the parameters γ, J_1 and J_0 by direct numerical integration. Concerning the impact of the chain length N we refer to Ref. [13]. We determine the maximal concurrence $C_{1,N}^{\max}$ that can be obtained within the time interval $T = [0, \ldots, 4N/\max(J_0, J_1)]$. The results depicted in Fig. 1(a) reveal that at $\omega_d = 2h_0$ the maximal concurrence assumes a value close to unity during this time interval and is significantly larger than for other frequencies. We refer to this resonance condition as *entanglement resonance*, which holds independently of the other parameters. On the contrary, we find that the height and width of the resonance peak depend on the intensities J_0 and J_1 and on the chain length N (not shown in the figure, see Refs. [13]). We also notice the existence of a secondary, smaller peak at the driving frequency $\omega_d = h_0$. In contrast to the main peak, its amplitude strongly decreases with the coupling intensity and increasing chain length [13].
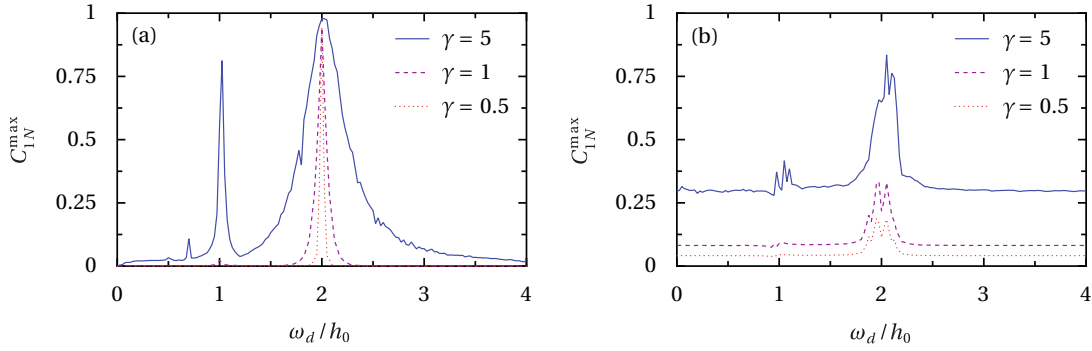
Fig. 1. Maximal concurrence C_{1N}^{max} between the end spins as a function of the driving frequency for various anisotropies. (a) Entanglement creation by modulation of the interaction $J(t)$ with the parameters $h_1 = 0$, $J_0 = 0$, and $J_1 = 0.1h_0$, cf. Eq. (2). (b) Corresponding effect due to modulation of the Zeeman fields $h_n(t)$, for $h_1 = 0.1h_0$, $J_0 = 0.1h_0$, and $J_1 = 0$. The chain length is $N = 6$ in both cases.

In order to understand this phenomenon quantitatively, we replace the Hamiltonian (3) by its time average within a rotating-wave approximation (RWA). At the resonance condition $\omega_d = 2h_0$, we obtain

$$\widetilde{H}_R = \frac{J_0}{2} \sum_{n=1}^{N-1} \left[\sigma_n^+ \sigma_{n+1}^- + \tilde{\gamma}\sigma_n^+ \sigma_{n+1}^+ + \mathrm{h.c.} \right], \tag{7}$$

with the effective anisotropy $\tilde{\gamma} = \gamma J_1 / 2J_0$. This means that for resonant driving, the time-dependent XY-model (1) can be mapped to the static XY-model (7) without Zeeman fields. In both cases, the entanglement generated between the two ending spins is maximal and controlled by the parameter $\tilde{\gamma}$ and the chain length N. Note that $J_0 \to 0$ corresponds to the infinitely anisotropic limit $\tilde{\gamma} \to \infty$. One important point is worth being mentioned: the concurrence approaches unity in the limit of vanishing J_0, i.e. for infinite $\tilde{\gamma}$. In this limit, the amount of entanglement no longer depends on J_1 and γ. An argumentation given in Ref. [13] explains why the limit $J_0 \to 0$ is optimal for entanglement generation. As a rule of thumb, the concurrence becomes maximal when minimizing the swap terms in the Hamiltonian (3). Let us finally mention that in Ref. [13], the entanglement scalability with the chain length N and the arrival time for this entanglement was studied.

3.2 Modulation of the local fields

In the following, we investigate the response to driving with local fields. We assume that at $t = 0$ the interaction is switched to a constant value with $J_0 > 0$, $J_1 = 0$. However, the local Zeeman field has now both ac and dc contributions, $h(t) = h_0 + h_1 \sin(\omega t)$. Again we assume a homogeneous chain, $\epsilon_j = 1$ for all j. Proceeding exactly as above, we compute the maximum concurrence reachable within the time interval $[0, \ldots, 4N/\max(J_0, J_1)]$. Our numerical results are drawn in Fig. 1(b). Also in this case we find an entanglement resonance for $\omega_d = h_0$ and for $\omega_d = 2h_0$, where the peak at $\omega_d = 2h_0$ dominates clearly. In order to understand this behavior we recall the Hamiltonian in the interaction picture, Eq. (3), simplified by setting $J_1 = 0$ in this case,

$$H = \frac{J_0}{2} \sum_{n=0}^{N-1} \left[\sigma_n^+ \sigma_{n+1}^- + \sigma_n^- \sigma_{n+1}^+ + \gamma \Big(\mathrm{e}^{\mathrm{i}\Sigma(t)} \sigma_n^+ \sigma_{n+1}^+ + \mathrm{e}^{-\mathrm{i}\Sigma(t)} \sigma_n^- \sigma_{n+1}^- \Big) \right] \tag{8}$$

with $\Sigma(t) = 2\int_0^t \mathrm{d}s (h_0 + h_1 \sin(\omega_d t))$. Notice that the driving no longer affects the swapping terms. On the other hand, the entanglement in terms of the concurrence is favored by the terms $\sigma_n^+ \sigma_{n+1}^+ + \mathrm{h.c}$, as pointed out after Eq. (3). For this reason, the resonances should assume values for which the time-dependent coefficients $\exp[\mathrm{i}\Sigma(t)]$ are not averaged to zero. To get further
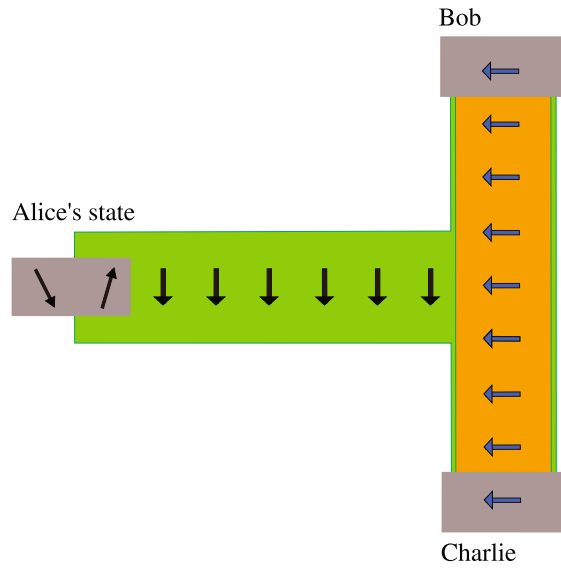
Fig. 2. Model for the simplest quantum router possible. A green spin chain allows perfect transfer and is not driven, while the propagation in the orange chain is controlled by ac fields.
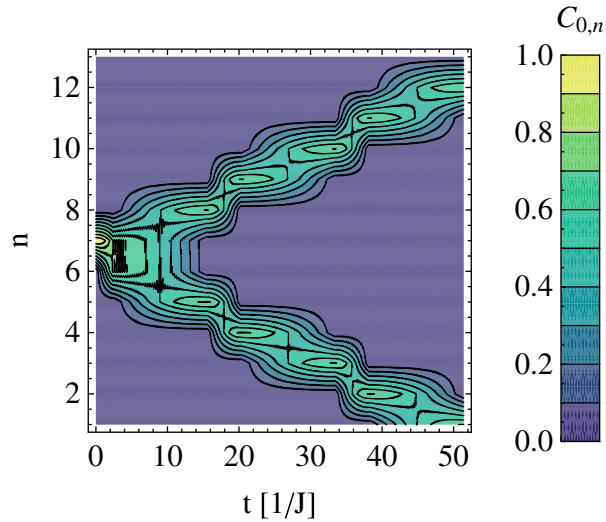

Fig. 3. Entanglement transport in a spin chain structure corresponding to Fig. 2. Concurrence $C_{0,n}$ [Eq. (5)] between the spin at Alice's site in the horizontal chain (labeled here $n = 0$) and the spins in the vertical chain. The entanglement is split up, arriving both Bob ($n = 12$) and Charlie ($n = 1$) after a given time. Here, the chain is isotropic ($\gamma = 0$), while the Zeeman fields have a ratchet-like globally driven shape as described in Ref. [1].

insight, we perform a Taylor expansion in powers of (h_1/ω), yielding

$$
\mathrm{e}^{\mathrm{i}\Sigma(t)} = \mathrm{e}^{\mathrm{i}h_1/\omega_d} \sum_n (-\mathrm{i})^n \left(\frac{h_1}{\omega_d} \right)^n \frac{1}{n!} \sum_k \binom{n}{k} \mathrm{e}^{\mathrm{i}[2h_0 + (n-2k)\omega_d]t} \tag{9}
$$

where $\binom{n}{k} = n!/k!(n-k)!$ are binomial coefficients. With this at hand we obtain the resonance condition

$$
2h_0 + (n - 2k)\omega_d = 0 \tag{10}
$$

To lowest order, Eq. (10) is fulfilled for $n = 1$, which yields $\omega_d = 2h_0$. This again confirms our numerical results depicted in Fig. 1. The next order at $n = 2$ yields the second resonance
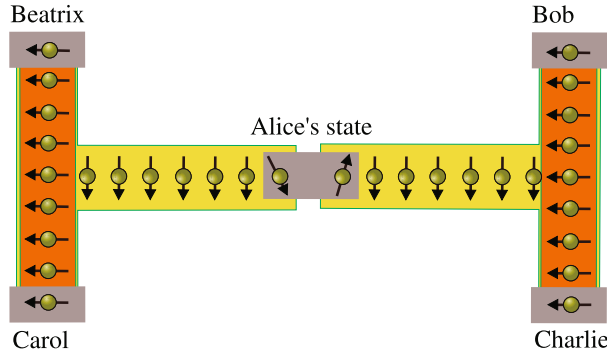
Fig. 4. Setup for the production of quadripartite distant entangled state, where Alice sends here initial singlet into two different driven chains which both are in operated in the splitting mode.

condition $\omega_d = h_0$, which explains the second peak in the figure. Peaks corresponding to resonances of higher orders ($n > 2$) are suppressed for $h_1/\omega_d \ll 1$.

Finally, we emphasize that the swapping terms $\sigma_n^+ \sigma_{n+1}^-$ are unaffected by driving the local fields. Thus, less concurrence is obtained as compared to the case with time-dependent interaction described in Sec. 3.1. This feature becomes apparent when comparing the Hamiltonians (7) and (9) or, equivalently, Figs. 1(a) and 1(b).

4 Steering of entanglement current via ac-control

In Ref. [1] the intriguing possibility of entanglement steering in an isotropic XY chain ($\gamma = 0$) was explored. It was shown how to make excitations in the spin chain propagate into a specific direction with a ratchet-like profile of the local Zeeman fields [23] plus a superimposed oscillation. This suggests the fabrication of a "quantum router". In this way, distant parties could be brought to share a high amount of entanglement, provided that decoherence is sufficiently small. As a further option, the excitation may be split into two parts, each propagating to one end of the chain. This results in entangling three distant parties rather than two. In Fig. 2 we sketch a model for the simplest router possible, where the entanglement has two possibilities of propagation. Corresponding numerical results about splitting of entanglement into two directions are depicted in Fig. 3.

To extend and generalize this elementary sketch of a quantum router, we point out how multipartite entanglement could be created between many distant parties. For this purpose, we suggest choosing a setup in which the entanglement signal has been sent through a driven spin chain, split in two. Both tail ends of the chain get thus entangled with the sender of the packet. The initial state $|100\rangle$ having been sent by Alice, the final state becomes

$$|\text{Alice, Bob, Charlie}\rangle = \frac{1}{\sqrt{2}}\left[|100\rangle + \frac{1}{\sqrt{2}}\left(|010\rangle + |001\rangle\right)\right], \qquad (11)$$

and is now shared by Alice, Bob and Charlie (the entries of the state vectors are given in this order). State (11) is a tripartite entangled state with similarity to a W-state [24,25], except for the weighting factors. It represents the different quantum coherent histories, i.e. outcome possibilities of excitation transfer. The component $|100\rangle$ refers to the case in which Alice has not sent any excitation through the driven chain. The latter two terms $|010\rangle$ and $|001\rangle$ result from splitting an excitation, which has been sent by Alice before.

If other driven chains are appended to Bob and Charlie, initial excitations can be split further. This results in a final penta-partite entangled state, i.e. a state held between five parties, which exhibits yet two more terms. However, the share of the distant parties gets diluted by a factor $1/\sqrt{2}$ every time the signal is split, while Alice's fraction never gets diminished. To get over this drawback, Alice can send her excitation to another spin array in a different direction. As illustrated in Fig. 4, this would result in a quadripartite state, where Bob and Charlie are
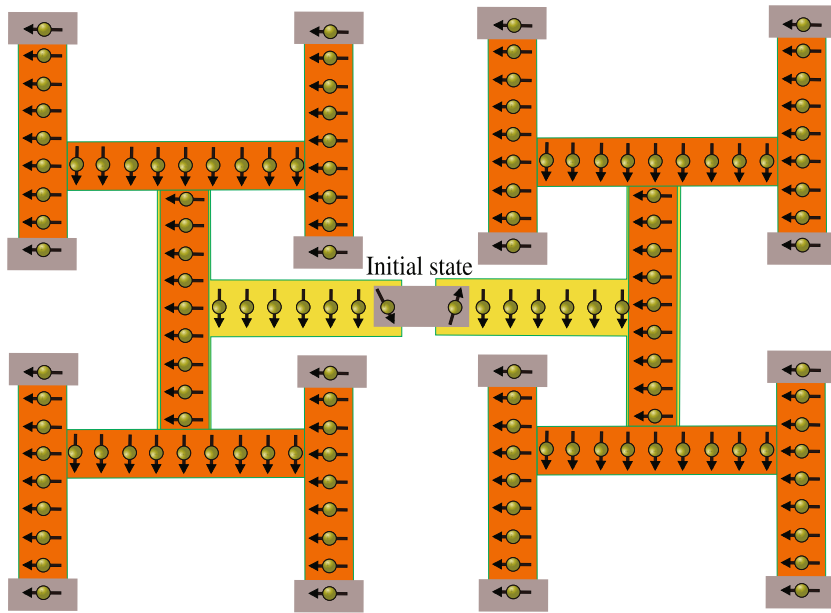
Fig. 5. Setup for the production of multipartite (sixteen parties) distant entangled states where Alice's singlet is split several times. As above the gray boxes mark output terminals.

entangled with Beatrix and Carol,

$$|\text{Beatrix, Carol, Bob, Charlie}\rangle = \frac{1}{2}\big[|1000\rangle + |0100\rangle + |0010\rangle + |0001\rangle\big]. \qquad (12)$$

This state is well balanced, and further splittings keep this balance unaffected if performed symmetrically on both ends. We notice too that the cardinality of the states is now even, whereas it is odd in the above scenario. To exploit advantages of multipartite distant entangled states, one could use a setup such as sketched in Fig. 5.

5 Experimental realizations and decoherence effects

A highly accurate and stable confinement of ions in traps has been achieved in the last decade, together with the possibility of operating in the ground state of the spatial ionic motion [26,27]. Several proposals to use this amazing tools in order to simulate spin chains have been given [4,37]. Here, the use of magnetic field gradients and state dependent laser forces, respectively, yield an effective spin-spin coupling mediated by the spatial degrees of freedom. The latter is achieved through Coulomb repulsion between ions [28], or a wire-mediated capacitive coupling of the ions residing in neighboring traps [29]. These proposals allow for the accurate simulation of many spin Hamiltonians, included Eq. (1), provided the mean photon numbers (temperatures) with respect to the relevant degrees of freedom are low. It must be noted that in [4] spins as such are used indeed, whereas in [37] they are simulated by means of two internal electronic ion levels. The latter proposal has been experimentally realised [38]. Furthermore, the first two Fock levels of the axial motion can be used to implement spins for the purpose of quantum routing [1], given that the ions in the chain can be prepared in the ground state with a probability of 99.9% [26].

In the following, we take into account decoherence, which is the main obstacle for the creation of entanglement through resonant driving. It originates from weak but unavoidable coupling of the spin chain to a typically large number of uncontrollable external degrees of freedom. Irrespective of its physical nature, the environment is usually modeled as a bath of harmonic oscillators, each coupling to a system coordinate via its position operator [30–33].
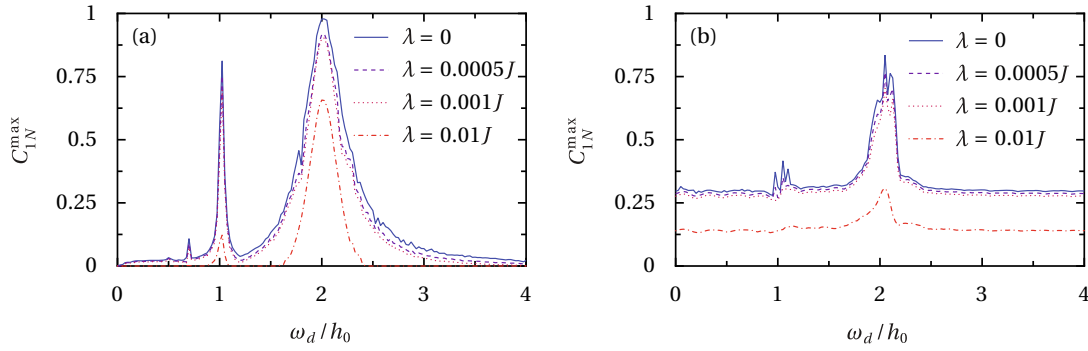
Fig. 6. Maximal concurrence $C_{1N}^{\max}$ for resonant driving (Eq. (2)) as a function of the driving frequency for various decoherence rates. The anisotropy parameter is $\gamma = 5$, while the chain length is $N = 6$. (a) Modulation of the interaction $J(t)$ with the parameters $h_1 = 0$, $J_0 = 0$, and $J_1 = 0.1h_0$. (b) Modulation of the fields $h_n(t)$, where $h_1 = 0.1h_0$, $J_0 = 0.1h_0$, and $J_1 = 0$.

Here we assume that each qubit n undergoes pure and independent dephasing, i. e. that its coordinate σ_n^z couples to a separate bath.

For weak dissipation, one can eliminate the bath within second-order perturbation theory and derive a Bloch-Redfield master equation for the reduced density operator ρ of the qubits [34]. Considering only phase noise on the traps, the equation takes a Lindblad form [35],

$$\dot{\rho} = -\frac{i}{\hbar}[H,\rho] + \frac{\lambda}{2}\sum_{n=1}^{N}(\sigma_n^z\rho\sigma_n^z - \rho), \tag{13}$$

where we have assumed that the effective decoherence rate λ is the same for all qubits. The above master equation has been obtained perturbatively in the dissipation strength. However, it turns out to be valid beyond the perturbative regime and therefore provides an accurate description of the dephasing dynamics [36]. The heating rate, which would include relaxation terms in the master equation, is typically several orders of magnitude smaller than the dephasing rate. This justifies the modelling of decoherence by pure phase noise. We use a rather conservative estimate and assume $\lambda \sim 10^{-4}J$.

Now we consider the impact of decoherence in the resonance phenomena discussed in Sec. 3. In Fig. 6 we plot the concurrence versus the frequency at different decoherence rates. Obviously, the concurrence becomes smaller with increasing decoherence. This reduction is related to the quantum master equation (13) with respect to the time it takes for the entanglement signal to reach the ends of the chain. Even so, the entanglement is well preserved for a decoherence rate $\lambda = 0.001J$. This is quite a realistic estimate for most physical systems that are suitable for experimental verification of entanglement resonance. For this reason, it should be possible to observe entanglement transport in an experiment as proposed, even though it will be limited by decoherence.

6 Conclusions

The transfer of methods established in condensed matter physics to the field of quantum information, and vice versa, has recently undergone a blossoming and promoting activity [39]. With this work, we have reviewed and extended our proposals [1,13] for generating and routing entanglement in a spin chain by utilizing time-dependent control of spin-spin interactions. Entanglement routing is achieved by a global manipulation of the chain via external driving fields. This method possesses a salient advantage as compared to the rather difficult local addressing of individual spins, since that task requires a delicate tuning of intrinsic system parameters. An optimal amount of entanglement is generated at a particular resonance, which builds a bridge to the familiar theory of coherent destruction of tunneling [32,40,41].

Thus, driving with external fields paves the way to control entanglement dynamics in realistic spin chains. We further elaborated on the role of decoherence thereby incorporating the unavoidable influence of environmental degrees of freedom in a realistic scenario. With regard to an experimental realization, we have sketched the implementation with Penning traps. Another possibility consists in using tailored Josephson junction arrays.

A further advantage of our time-dependent driving scheme is the substantial decoherence suppression by use of ac-fields [32, 42–44]. This time-dependent manipulation allows the optimal control in attaining maximal entanglement of distant objects [13]. In addition, Landau-Zener dynamics has been proposed as well for entanglement generation protocols [45, 46]. Finally, the implementation of optimal quantum gates was suggested [47]. All in all, this justifies the efforts in employing the toolboxes from both driven quantum systems and solid state correlation physics in administrating quantum information processing.

References

1. D. Zueco, F. Galve, S. Kohler, P. Hänggi, Phys. Rev. A **80**, 042303 (2009)
2. R.M. White, *Quantum Theory of Magnetism*, 2nd edn. (Springer, Berlin, 1983)
3. I. Bloch, J. Dalibard, W. Zwerger, Rev. Mod. Phys. **80**, 885 (2008)
4. G. Ciaramicoli, I. Marzoli, P. Tombesi, Phys. Rev. A **78**, 012338 (2008)
5. G. Wendin, V.S. Shumeiko, in *Handbook of Theoretical and Computational Nanotechnology*, Vol. 3, edited by M. Rieth, W. Schommers (American Scientific Publishers, Los Angeles, 2006), p. 223
6. V.M. Kenkre, J. Phys. Chem. B **104**, 3960 (2000)
7. W. Nolting, *Quantum Theory of Magnetism* (Springer, New York, 2009)
8. V. Giovannetti, S. Lloyd, L. Maccone, Science **306**, 1330 (2004)
9. L. Amico, R. Fazio, A. Osterloh, V. Vedral, Rev. Mod. Phys. **80**, 517 (2008)
10. S. Bose, Phys. Rev. Lett. **91**, 207901 (2003)
11. D. Burgarth, Ph.D. thesis, University College London (2006), [`arXiv:0704.1309`] [quant-ph]
12. S. Bose, Contemp. Phys. **48**, 13 (2007)
13. F. Galve, D. Zueco, S. Kohler, E. Lutz, P. Hänggi, Phys. Rev. A **79**, 032332 (2009)
14. G. Burlak, I. Sainz, A.B. Klimov, Phys. Rev. A **80**, 024301 (2009)
15. J.F. Leandro, A.S.M. de Castro, F.L. Semião, [`arXiv:0909.3545`] [quant-ph] (2009)
16. X. Wang, A. Bayat, S.G. Schirmer, S. Bose, Phys. Rev. A **81**, 032312 (2010)
17. C. DiFranco, M. Paternostro, M.S. Kim, Phys. Rev. A **81**, 022319 (2010)
18. O. Romero-Isart, J.J. García-Ripoll, Phys. Rev. A **76**, 052304 (2007)
19. E. Lieb, T. Schultz, D. Mattis, Ann. Phys. **16**, 407 (1961)
20. H.J. Mikeska, W. Pesch, Z. Phys. B **26**, 351 (1977)
21. W.K. Wootters, Phys. Rev. Lett. **80**, 2245 (1998)
22. H. Wichterich, S. Bose, Phys. Rev. A **79**, 060302(R) (2009)
23. P. Hänggi, F. Marchesoni, Rev. Mod. Phys. **81**, 387 (2009)
24. W. Dür, G. Vidal, J.I. Cirac, Phys. Rev. A **62**, 062314 (2000)
25. P. Walther, K.J. Resch, A. Zeilinger, Phys. Rev. Lett. **94**, 240501 (2005)
26. C. Roos, T. Zeiger, H. Rohde, H.C. Nägerl, J. Eschner, D. Leibfried, F. Schmidt-Kaler, R. Blatt, Phys. Rev. Lett. **83**, 4713 (1999)
27. D. Leibfried, R. Blatt, C. Monroe, D. Wineland, Rev. Mod. Phys. **75**, 281 (2003)
28. G. Ciaramicoli, I. Marzoli, P. Tombesi, Phys. Rev. Lett. **91**, 017901 (2003)
29. S. Stahl, F. Galve, J. Alonso, S. Djekic, W. Quint, T. Valenzuela, J. Verdu, M. Vogel, G. Werth, Eur. Phys. J. D **32**, 139 (2005)
30. V.B. Magalinskii, Zh. Eksp. Teor. Fiz. **36**, 1942 (1959); Sov. Phys. JETP **9**, 1381 (1959)
31. A.O. Caldeira, A.L. Leggett, Ann. Phys. (N.Y.) **149**, 374 (1983)
32. M. Grifoni, P. Hänggi, Phys. Rep. **304**, 229 (1998)
33. P. Hänggi, G.L. Ingold, Chaos **15**, 026105 (2005)
34. K. Blum, *Density Matrix Theory and Applications*, 2nd edn. (Springer, New York, 1996)
35. G. Lindblad, Commun. Math. Phys. **48**, 119 (1976)

36. R. Doll, D. Zueco, M. Wubs, S. Kohler, P. Hänggi, Chem. Phys. **347**, 243 (2008)
37. D. Porras J.I. Cirac, Phys. Rev. Lett. **92**, 207901 (2004)
38. A. Friedenauer, H. Schmitz, J.T. Glueckert, D. Porras T. Schaetz, Nat. Phys. **4**, 757 (2008)
39. S. Schenk, G.L. Ingold, Phys. Rev. A **75**, 022328 (2007)
40. F. Grossmann, T. Dittrich, P. Jung, P. Hänggi, Phys. Rev. Lett. **67**, 516 (1991)
41. F. Grossmann, P. Jung, T. Dittrich, P. Hänggi, Z. Phys. B **84**, 315 (1991)
42. M. Grifoni, M. Sassetti, P. Hänggi, U. Weiss, Phys. Rev. E **52**, 3596 (1995)
43. M. Grifoni, M. Sassetti, U. Weiss, Phys. Rev. E **53**, R2033 (1996)
44. G. Kurizki, A.G. Kofman, D. Petrosyan, T. Opatrný, J. Optics B **4**, 294 (2002)
45. M. Wubs, S. Kohler, P. Hänggi, Physica E **40**, 187 (2007)
46. D. Zueco, G.M. Reuther, P. Hänggi, S. Kohler, Physica E **42**, 363 (2010)
47. K.M. Fonseca-Romero, S. Kohler, P. Hänggi, Phys. Rev. Lett. **95**, 140502 (2005)